COHERENCE AND PHASE NOISE IN SOFTWARE-DEFINED RADIO-BASED ICE-PENETRATING RADAR INSTRUMENTS

Thomas O. Teisberg¹, Dustin M. Schroeder^{1,2}, Anna L. Broome¹, Riley Culberg³

Department of Electrical Engineering, Stanford University,
 Department of Geophysics, Stanford University,
 Department of Earth and Atmospheric Sciences, Cornell University

ABSTRACT

Ice-penetrating radar (IPR) instruments are a widely used tool to understand the structure and dynamics of Earth's ice sheets and glaciers. Originally primarily designed to image the bedrock beneath ice, IPR systems are now being used for a wider range of scientific investigations. At the same time, new hardware architectures and customized radar systems are emerging. This combination of factors makes it worth re-visiting common assumptions about the noise characteristics of IPR systems and the phase coherence of measured reflections. In this work, we explore what it means for an IPR instrument to be coherent, how architectural choices in the design of software-defined radio-based instruments may impact phase coherence, and what instrument specifications should be considered for IPR applications that rely on measurements of small phase changes.

Index Terms— Ice-penetrating radar, phase noise, coherence, software-defined radio

1. INTRODUCTION

Ice-penetrating radar (IPR) systems are the primary geophysical instrument used to map englacial layering, englacial and subglacial hydrologic conditions, and bed topogography beneath Earth's ice sheets and glaciers. IPR systems are radar instruments designed primarily to image targets within or beneath large bodies of ice. Most instruments designed for coherent post-processing emit a frequency-swept, or chirped, signal, similar to frequency-modulated, continuous wave (FMCW) radars. Unlike true FMCW radar systems, however, most IPRs operate at less than 100% duty cycles, a trade-off that eliminates ambiguity in which transmitted pulse produced each reflection at some expense to the signal-to-noise ratio (SNR).

Attenuation rates in terrestrial glacial ice increase significantly with frequency [1], setting the upper frequency limit for most IPR systems well below 1 GHz, with some systems

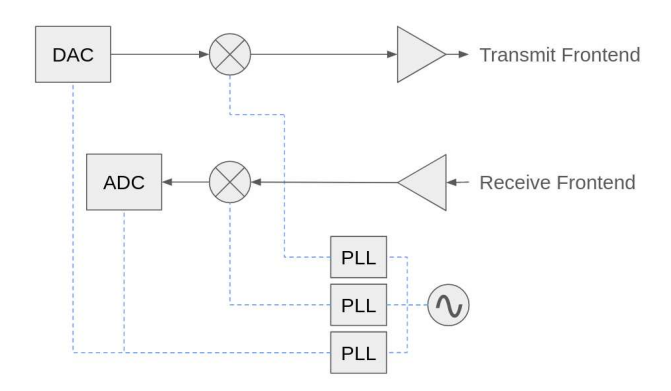


Fig. 1. Modern SDR architectures often use a single reference oscillator from which multiple software configurable frequency signals are derived. A conceptual diagram of one such architecture is shown here.

operating as low as 1 MHz center frequency. At these low frequencies, practical antenna design typically limits the system bandwidth to at most hundreds of megahertz and, in some cases, to only kilohertz. Recent advances in RF integrated circuits combined with these comparatively low center frequencies and bandwidths have opened up an extremely wide range of radar system architectures, including various systems based on software-defined radios (SDRs) [2] [3] [4].

Although conceptually similar to earlier radar systems, these SDR-based designs often incorporate software-configurable clocks, which motivates our review of phase noise in these systems. A diagram of the oscillators and clock signals for a common SDR configuration is shown in Figure 1.

The emergence of new IPR instruments has been encouraged by a range of new applications for these systems. While the early motivations for IPR surveys focused on mapping the approximate basal topography beneath glaciers and ice sheets, there are now a wider range of interests, including measuring small-scale vertical motion through interferometry [5], high-resolution across-track "swath" mapping [6], and time-series sub-glacial hydrology measurements [7].

A common feature of these applications is that they rely

T. O. T. was supported by a NASA FINESST Grant (80NSSC23K0271). A. L. B. was supported by NDSEG. Additional support was provided by the TomKat Center for Sustainable Energy and Stanford Data Science.

on accurate phase measurements of reflected signals. Thus they require "coherent" radar systems.

In this work, we propose a metric to quantify how "coherent" an IPR instrument is in a particular configuration. We then explore sources of phase noise in radar systems, with a particular focus on SDR-based IPR systems. Finally, we suggest design considerations for SDR-based IPR developers.

2. COHERENT RADAR SYSTEMS

Early uses of the term "coherent" in IPR contexts primarily treated it as a binary distinction. For example, a 2005 radar system description paper states:

"Early ice-sounding radar systems typically used incoherent receivers that only detected the power (or amplitude) of the radar signals. [...] A coherent radar system detects both the amplitude and phase of the radar signals and has a number of advantages over incoherent radar systems. For example, coherent signal integration from a moving airborne platform forms a synthetic aperture radar (SAR) that improves along-track resolution." [8]

This statement is clear in the context of other radar systems that record only the magnitude of the received signal. Such systems are, however, increasingly uncommon. New radar architectures are challenging the concept of coherence in different ways. For example, a recent paper describes a system in which "the individual hardware used for the transmitter and receiver is incoherent from each other, so we created a coherent system by exploiting the signal direct path to synchronize the devices" [9]. This paper also notes an expected gain in SNR for a coherent system linearly related to the number of pulses stacked.

Although multiple definitions of SNR exist, the most common is the ratio of the power in the desired part of the signal to the power in the noise component of the signal:

$$SNR = \frac{P_{\text{signal}}}{P_{\text{noise}}} \tag{1}$$

A common technique in IPR to improve SNR is known as stacking (generally) or coherent integration (when performed on a coherent system). Stacking involves averaging received samples from multiple pulses such that they add in phase, while any incoherent parts of the signal are gradually cancelled out through destructive interference.

$$x_{\text{stacked}}(t) = \frac{1}{n_{\text{stack}}} \sum_{n=1}^{n_{\text{stack}}} x \left(t + n \cdot \text{PRI} \right)$$
 (2)

Where PRI is the pulse repetition interval (or spacing in time between successive pulses). Achieving the desired linear increase in SNR with $n_{\rm stack}$ requires that the signal power remains constant and that the noise power decreases linearly.

Cases where the noise power does not decrease linearly may be related to a coherent noise source in the system. This can come from many different sources, such as clocks and power supplies. By some definitions, clutter may also be viewed as a source of target-dependent coherent noise.

Decreases in the signal power over increasing integration times can also occur. This phenomenon is more directly related to the concept of radar coherence. If anything alters the transmitted signal or how the signal is received, the digitized signal will not be identical in each recording, thus destructive interference may occur, reducing the signal power after stacking. We suggest that the reduction in signal power from a single chirp to a stacked sum over varying integration times is a useful metric to quantify the coherence of an IPR instrument. The upper bound of useful integration times is set by the period of time over which an IPR system could reasonably be expected to be observe the same reflectors. This could vary from seconds (for an airborne system) to days (for a static installation).

To build intuition about this metric, consider one possible source of such variations in a radar system. Many IPR instruments use an RF mixer to translate a signal produced at baseband to a carrier frequency. If the local oscillator used as the second input to the mixer contains some phase noise, this phase noise is added in to the transmitted signal. (Almost all mixer-based architectures use a mixer on the receiver as well. This is addressed in Section 4.)

Figure 2 shows the results of bandpass filtering a synthetic phase noise distribution with three different filters in order to visualize the impact on coherence of different spectral components of the phase noise distribution. Note than when most of the energy in the phase noise spectrum is concentrated well above the effective pulse repetition frequency (after stacking), there is no additional signal power loss from stacking. Although the phase noise contributes to the noise floor of the radar, it can effectively be treated similarly to other noise sources. For a system designer, the important specification is to keep the phase noise profile low beneath the effective pulse repetition frequency.

3. PHASE NOISE OVERVIEW

The output of an oscillator, such as the one shown in Figure 1, can be modelled as a sine wave of some amplitude A and frequency f, with small noise terms added into both of these components [10]:

$$s(t) = A(1 + n(t))\cos(2\pi f t + \phi(t))$$
 (3)

Where n(t) is zero-mean noise representing amplitude fluctuations and $\phi(t)$ is the phase noise. We will ignore the amplitude fluctuations and focus on the phase noise portion of this. The power spectral density of $\phi(t)$ may be approximately white at large frequency offsets but is characterized by

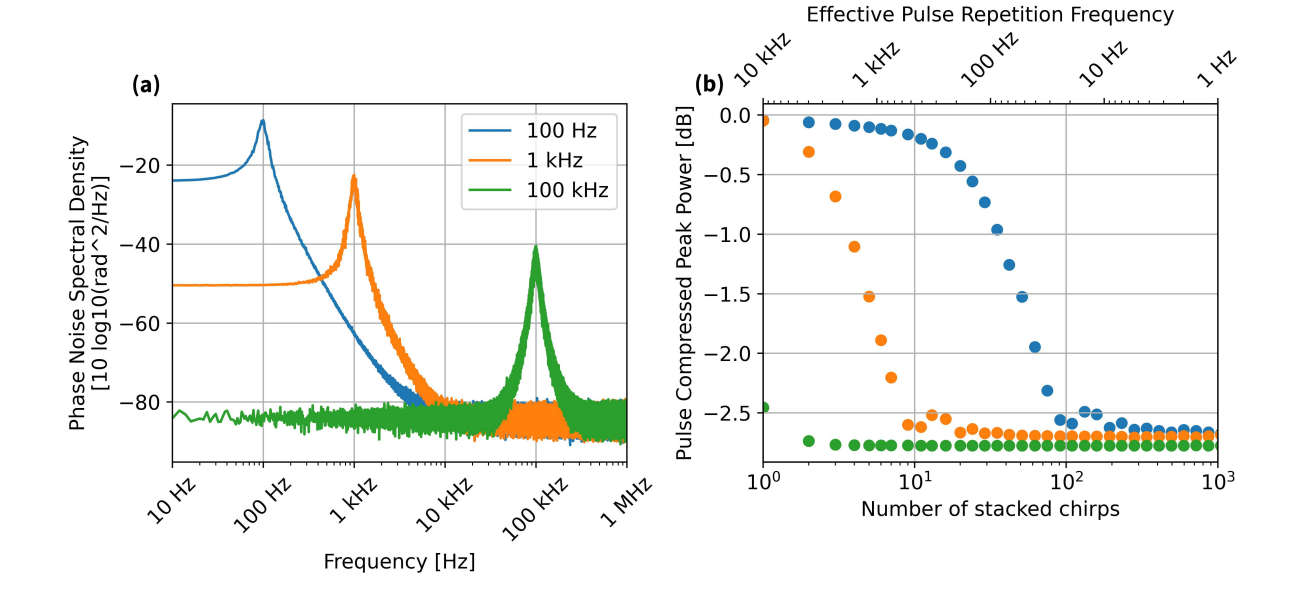


Fig. 2. (a) Phase noise spectral densities for three synthetic phase noise distributions, designed to illustrate the effects of phase noise at differing frequencies. (b) Average signal peak power after pulse compression plotted against coherent integration time (number of stacks) for signals corrupted by each of the phase noise profiles.

1/f, $1/f^2$, and $1/f^3$ noise sources creating a peak at low offset frequencies [11]. These low-offset frequency noise contributions represent slowly varying phase terms that are added in to the radar signal in ADCs, DACs, and mixers.

SDR-based IPR architectures are also likely to incorporate multiple phase-locked loops (PLLs) used to generate configurable frequency clocks from a single frequency reference source, such as a crystal oscillator. In these cases, care must be taken to consider which parts of the phase noise spectra may be correlated. Though the details of PLLs will not be discussed here, the phase noise profile within the PLL loop bandwidth is typically an amplified version of the reference oscillator phase noise spectrum, scaled by $\left(\frac{f_{\text{output}}}{f_{\text{input}}}\right)^2$ [12]. Outside of the loop bandwidth, the phase noise is generally set by characteristics of the voltage-controlled oscillator and uncorrelated with the reference oscillator [12].

4. PHASE NOISE MODEL IN SDR-BASED IPR INSTRUMENTS

At baseband, a radar signal with IQ modulation can be represented as:

$$x_{\text{BB,TX}}(t) = e^{j\theta(t)} \tag{4}$$

 $\theta(t)$ represents the phase progression of the signal. If the DAC sample clock has non-zero phase noise, there will be some jitter in the timing of each sample. As a result, the actual signal produced by the DAC will be:

$$x_{\text{DAC}}(t) = e^{j\theta(t - t_{j}(t))}$$
 (5)

$$t_{\rm j}(t) = \frac{\phi_{\rm clock}(t)}{2\pi f_{\rm clock}} \tag{6}$$

 $t_{\rm j}$ is the instantaneous offset of the DAC's clock, which is related to the instantaneous phase offset of the clock $\phi_{\rm clock}(t)$ by the clock's nominal frequency $f_{\rm clock}$. This signal is then mixed with a local oscillator (LO) to upconvert the baseband signal to the carrier frequency. Ignoring losses, an ideal mixer can be modelled as a multiplication in the time domain:

$$x_{\text{output}}(t) = x_{\text{DAC}}(t) \cdot e^{2\pi f_{LO}t + \phi_{\text{LO,TX}}(t)}$$
 (7)

This signal travels to an antenna, reflects off of an object, and returns to the receiver's antenna after some propagation delay time $t_{\rm r}$. IQ downmixing and sampling at the ADC perform inverse processes to their transmit counterparts, leaving the signals:

$$x_{\text{BB,RX}}(t) = x_{\text{DAC}}(t - t_r) \times$$

$$e^{\phi_{\text{LO,TX}}(t - t_r) - \phi_{\text{LO,RX}}(t) - 2\pi f_{\text{LO}} t_r}$$
(8)

$$x_{ADC}(t) = x_{BB,RX}(t + t_i(t)) \tag{9}$$

$$x_{\text{ADC}}(t) = x_{\text{DAC}}(t + t_j(t) - t_r) \times$$

$$e^{\phi_{\text{LO,TX}}(t + t_j(t) - t_r) - \phi_{\text{LO,RX}}(t + t_j(t)) - 2\pi f_{\text{LO}} t_r}$$

$$(10)$$

$$x_{\text{ADC}}(t) = e^{j\theta(t + t_j(t) - t_r - t_j(t + t_j(t) - t_r))} \times e^{\phi_{\text{LO,TX}}(t + t_j(t) - t_r) - \phi_{\text{LO,RX}}(t + t_j(t)) - 2\pi f_{\text{LO}} t_r}$$
(11)

For a continuous wave radar (where $\theta(t)$ is a linear function), Equation 11 may be significantly simplified. While it cannot be as easily reduced for a chirped radar signal, the equation can easily be simulated for any radar signal.

To this point, we have assumed only the clock architecture of Figure 1. Specifically, we assumed that the ADC and DAC are clocked from the same source and thus experience the same time jitter $t_j(t)$. For the mixers, we assume that the center frequency $f_{\rm LO}$ is the same but not necessarily that the phase noises are identical.

The correlation between the two mixer LO phase noise terms depends strongly on the system architecture. For the architecture in Figure 1, we can assume they are correlated if the PLL loop bandwidth is significantly greater than the lowest desired pulse repetition frequency, such that higher frequency phase noise that might be uncorrelated will not impact the system coherence. If $\phi_{LO,RX}(t) = \phi_{LO,TX}(t)$, there is an interference effect between these two phase noise terms as a function of the delay time t_r , defined in the frequency domain by the transfer function:

$$|H(f)|^2 = 4\sin^2(\pi f t_r)$$
 (12)

For a derivation of this function, see [10]. For the following system example, we will assume $\phi_{LO,RX}(t) = \phi_{LO,TX}(t)$.

5. EXAMPLE SYSTEM SIMULATION

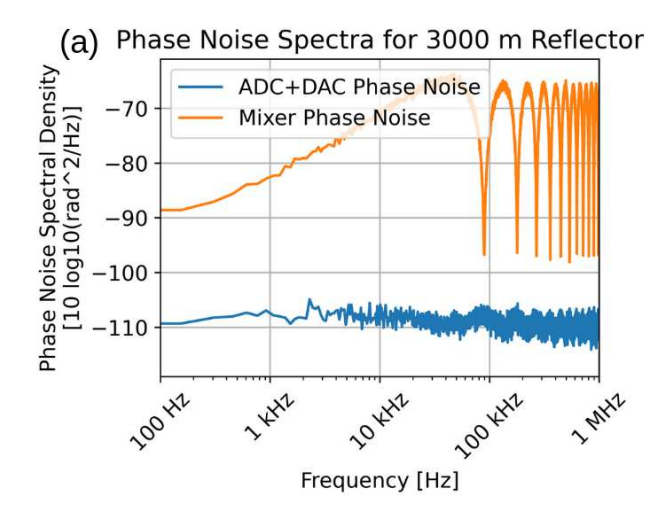
We consider an hypothetical example IPR system with a sampling frequency of 20 MHz, a 20 μ s chirp with a 10 MHz bandwidth centered at 400 MHz, and a pulse repetition interval of 100 μ s. The reference oscillator is a 40 MHz crystal with a synthetic phase noise spectrum made up of a sum of $1/f^2$, 1/f, and white noise.

Figure 3(a) shows the results of separately simulating the phase noise spectrum of the baseband and mixer phase noise contributions. For this relatively long reflection distance, the effects of equation 12 are clearly visible. Because all clocks are derived from the same 40 MHz reference oscillator but the mixer LO frequency is 20 times higher than the ADC/DAC clock rate, the starting phase noise spectral density is $\sim\!26~{\rm dB}$ higher. Under these typical circumstances ($f_{\rm LO}\gg f_{\rm clock}$ and both are derived from the same oscillator), the phase noise of the mixers dominates the overall spectrum.

This system would be considered a "coherent" radar by the classical binary definition. As shown in Figure 3(b), however, we can more specifically quantify how coherent it is as a function of the coherent integration time and expected reflection distance.

6. SUMMARY

"Coherent" has been used as a binary distinction in IPR systems for decades. For most applications, such radar systems



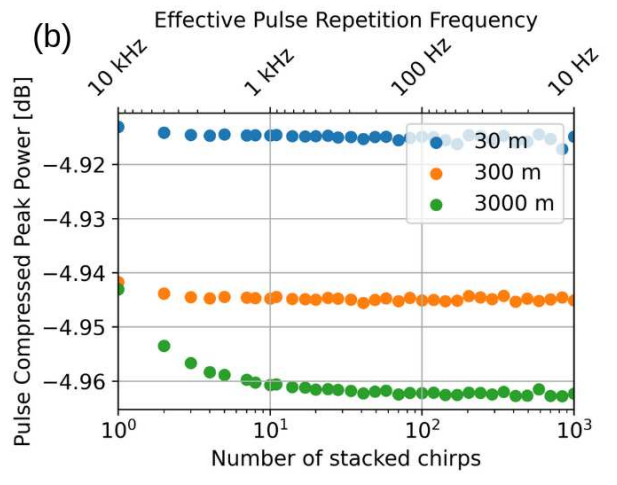


Fig. 3. (a) Simulated phase noise spectra for the two components of Equation 11 plotted for an example radar system. (b) Signal peak power versus coherent integration time for the same example system at three different reflector distances.

are approximately coherent and the term is suitable for the purpose. With an increasing focus on radar applications that rely on extremely precise phase measurements, it makes sense to carefully review internal sources of phase noise, especially for SDR-based radar systems that may contain more complex clock and oscillator designs.

We have introduced an approach to quantifying coherence for IPR systems and provided a model for analyzing and simulating phase noise in common IPR system architectures. Our results suggest that most SDR-based IPR systems are likely to be approximately coherent. For systems with potentially poor phase noise reference oscillators, with extremely narrow loop bandwidth PLLs, or with high fractional bandwidth, simulations such as those performed in Section 5 are critical to system design.

7. REFERENCES

- [1] J.D. Paden, C.T. Allen, S. Gogineni, K.C. Jezek, D. Dahl-Jensen, and L.B. Larsen, "Wideband measurements of ice sheet attenuation and basal scattering," *IEEE Geosci. Remote Sensing Lett.*, vol. 2, no. 2, pp. 164–168.
- [2] Anna L. Broome and Dustin M. Schroeder, "A radiometrically precise multi-frequency ice-penetrating radar architecture," *IEEE Trans. Geosci. Remote Sensing*, vol. 60, pp. 1–15.
- [3] Thomas O. Teisberg, Dustin M. Schroeder, Anna L. Broome, Franklin Lurie, and Dennis Woo, "Development of a UAV-borne pulsed ice-penetrating radar system," in *IGARSS* 2022 2022 IEEE International Geoscience and Remote Sensing Symposium. pp. 7405–7408, IEEE.
- [4] Peng Liu, Jesus Mendoza, Hanxiong Hu, Peter G. Burkett, Julio V. Urbina, Sridhar Anandakrishnan, and Sven G. Bilen, "Software-defined radar systems for polar ice-sheet research," *IEEE J. Sel. Top. Appl. Earth Observations Remote Sensing*, vol. 12, no. 3, pp. 803–820.
- [5] Jonathan Kingslake, Richard C. A. Hindmarsh, Gufinna Aalgeirsdóttir, Howard Conway, Hugh F. J. Corr, Fabien Gillet-Chaulet, Carlos Martín, Edward C. King, Robert Mulvaney, and Hamish D. Pritchard, "Full-depth englacial vertical ice sheet velocities measured using phase-sensitive radar: Measuring englacial ice velocities," *Journal of Geophysical Research: Earth Surface*, vol. 119, no. 12, pp. 2604–2618, Dec. 2014.
- [6] N. Holschuh, K. Christianson, J. Paden, R.B. Alley, and S. Anandakrishnan, "Linking postglacial landscapes to glacier dynamics usingswath radar at Thwaites Glacier, Antarctica," *Geology*, Jan. 2020.
- [7] Irena Vaňková, Denis Voytenko, Keith W. Nicholls, Surui Xie, Byron R. Parizek, and David M. Holland, "Vertical Structure of Diurnal Englacial Hydrology Cycle at Helheim Glacier, East Greenland," *Geophysical Research Letters*, vol. 45, no. 16, pp. 8352–8362, Aug. 2018.
- [8] Matthew E. Peters, Donald D. Blankenship, and David L. Morse, "Analysis techniques for coherent airborne radar sounding: Application to west antarctic ice streams," J. Geophys. Res., vol. 110, pp. 2004JB003222.
- [9] Nicole L. Bienert, Dustin M. Schroeder, Sean T. Peters, Emma J. MacKie, Eliza J. Dawson, Matthew R. Siegfried, Rohan Sanda, and Poul Christoffersen, "Postprocessing synchronized bistatic radar for long offset

- glacier sounding," *IEEE Trans. Geosci. Remote Sensing*, vol. 60, pp. 1–17.
- [10] Pieter W. van der Walt and Werner Steyn, "Characterizing phase noise in self-referencing radar," *IEEE Aerosp. Electron. Syst. Mag.*, vol. 38, no. 12, pp. 4–13.
- [11] Walt Kester, "Converting oscillator phase noise to time jitter," 2008, Analog Devices Tutorial MT-008.
- [12] Curtis Barrett, "Fractional/Integer-N PLL Basics," 1999, TI Publication SWRA029.